Supporting information

A programmable catalytic molecular nanomachine for highly sensitive proteins and small molecules detection

Na Li*, Minhui Li, Mei Li

Key Laboratory of Micro-Nanoscale Bioanalysis and Drug Screening of Guangxi Higher Education, School of Pharmacy, Guangxi Medical University, Nanning 530021, China

*E-mail: nali@hnu.edu.cn

Table S1. Sequences of synthesized DNA probes

Name	Sequence (5'-3')
I_a	CGACATCTAACCTAGC TCACGGA
H_a	TCCGTGA GCTAGGTTAGATGTCG CCATGTGTAGA CGACATCTAACCTAGC
H_b	AGATGTC GTCTACACATGG CGACATCTAACCTAGC CCATGTGTAGAC
I	TGTCATCTAACTAGT TCACGGA
H_{1a}	TCCGTGA ACTAGTTAGATGACA CCAATCTGTAC T GTCATCTAACTAGT
H_{2a}	AGATGAC AGTACAGATGG TGTCATCTAACTAGT C CATCTGTACT
H_{2b}	AGTTAGAT GACAGTACAGATGG TGTCATCTAACTA GT CCATCTGTACTGTC
H_{2c}	TAGTTAGA TGACAGTACAGATGG TGTCATCTAACT AGT CCATCTGTACTGTCA
H_{2d}	CTAGTTAG ATGACAGTACAGATGG TGTCATCTAAC TAGT CCATCTGTACTGTCAT
I_{b1}	Biotin-TTTTTTTTTTTTTTTTTTTTTTTTTTTTTTTTT TTTT GACAGG TT TCACGGA
I_{b2}	TGTCATCTAACTAGT CCTGTC TTTTTTTTTTTTTTT TTTT TTTTTTTTTTTTTTTTTT-Biotin
I_{D1}	Dig-TTTTTTTTTTTTTTTTTTTTTTTTTTTTTTTTTTT TT GACAGG TT TCACGGA
I_{D2}	TGTCATCTAACTAGT CCTGT CTTTTTTTTTTTTTTT TTTT TTTTTTTTTTTTTTTTTT-Dig
H_1	AGCCTCGTCGATCTCCACC TTTTT TCCGTGA ACT(F AM)AGTTAGATGACA CCAATCTGTAC TGTCATCTA ACTAGT(BHQ1)
H_2	AGCCTCGTCGATCTCCACC TTTTT CTAGTTAG ATG ACAGTACAGATGG TGTCATCTAACTAGT CCATCTG TACTGTCAT
Y_1	GGTGGAGATCGACGAGGCT GGAAGTGACTCATGTT AGCAGGTCTGTAAGTA
Y_2	GGTGGAGATCGACGAGGCT TACTTACAGACCTGCT A CATCCTGACAACTTAGT
Y_3	GGTGGAGATCGACGAGGC TACTAAGTTGTCAGGAT G AACATGAGTCACTTCC

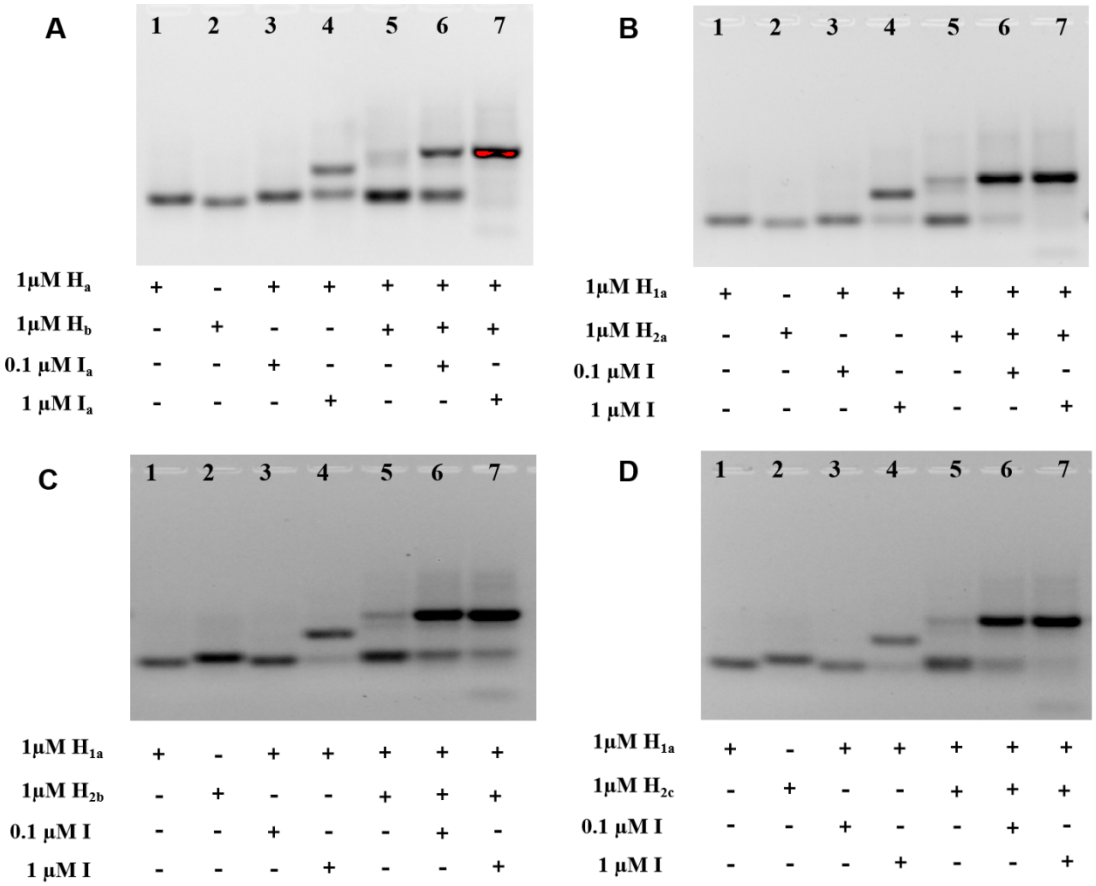

Fig. S1. Agarose gel electrophoresis image to test the efficiency of initiator triggered CHA between different hairpin probes in 1x HEPES buffer (20 mM HEPES, 12.5 mM $MgCl_2$, pH 8.0) at 37 °C for 4 h. (A) H_a and H_b. (B) H_{1a} and H_{2a}. (C) H_{1a} and H_{2b}. (B) H_{1a} and H_{2c}.

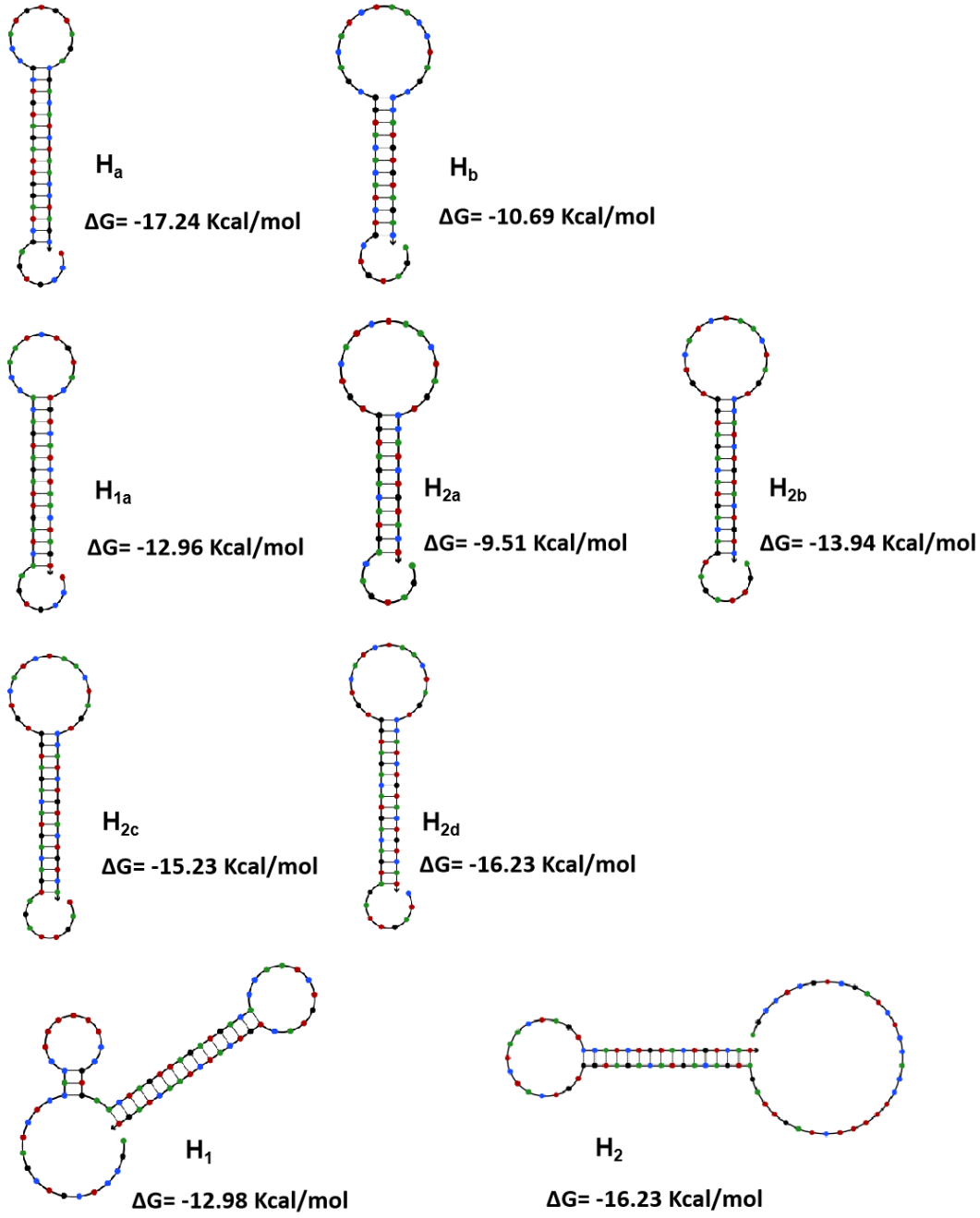

Fig. S2. The secondary structures and free energy (ΔG) values of hairpin probes were estimated (37°C) by NUPACK analysis.

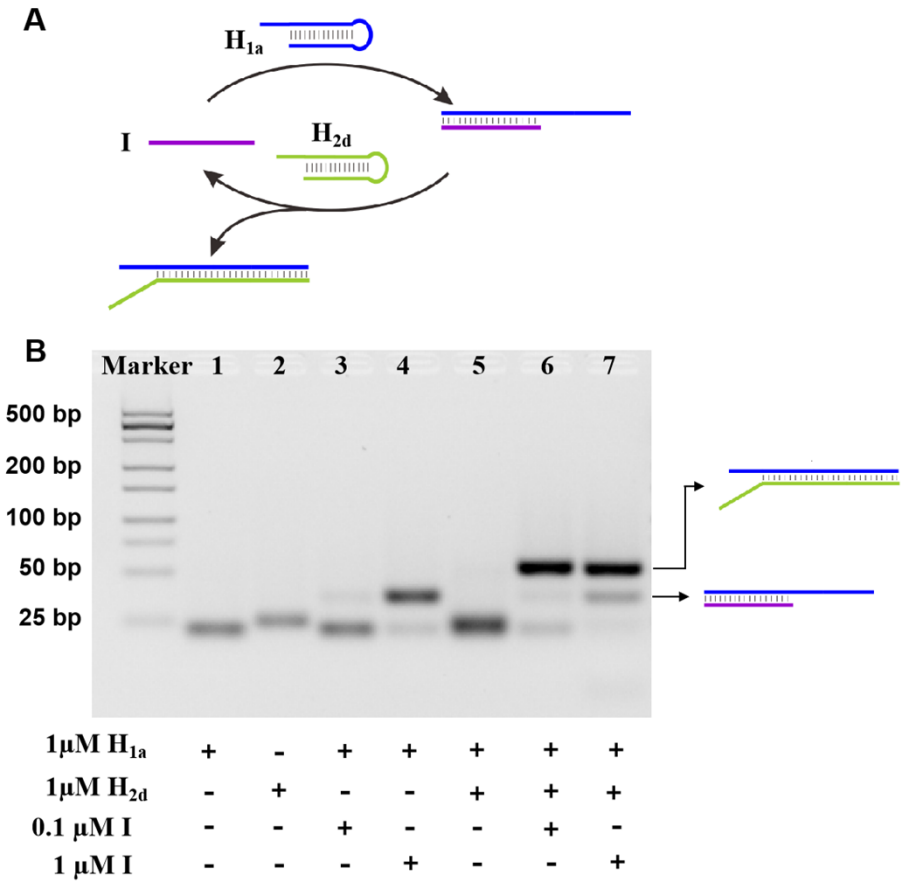

Fig. S3. (A) Principle illustration of the traditional CHA using hairpin H_{1a} and H_{2d}. (B) Agarose gel electrophoresis image to test the efficiency of initiator triggered CHA reaction between hairpin H_{1a} and H_{2d} in 1x HEPES buffer at 37 °C for 4 h.

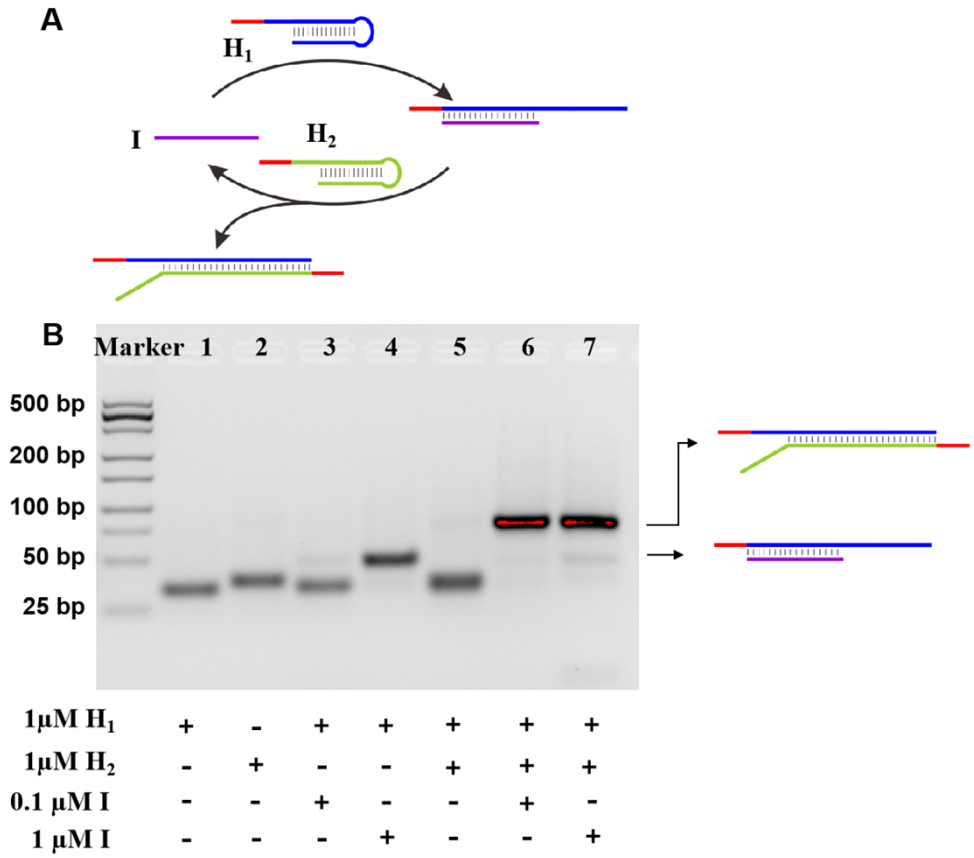

Fig. S4. (A) Principle illustration of the traditional CHA using hairpin H_1 and H_2. (B) Agarose gel electrophoresis image to demonstrate the efficiency of initiator triggered CHA reaction between hairpin H_1 and H_2 in 1x HEPES buffer at 37 °C for 4 h.

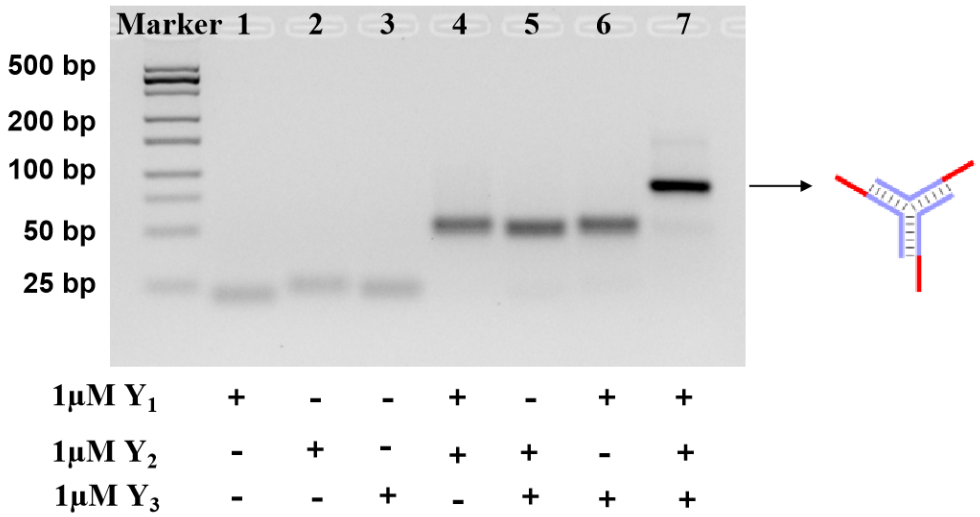

Fig. S5. Agarose gel electrophoresis image the assembly process of Y-shaped DNA using Y_1, Y_2, and Y_3 in 1x HEPES buffer at 37 °C for 1 h, the reaction conditions were shown in panel.

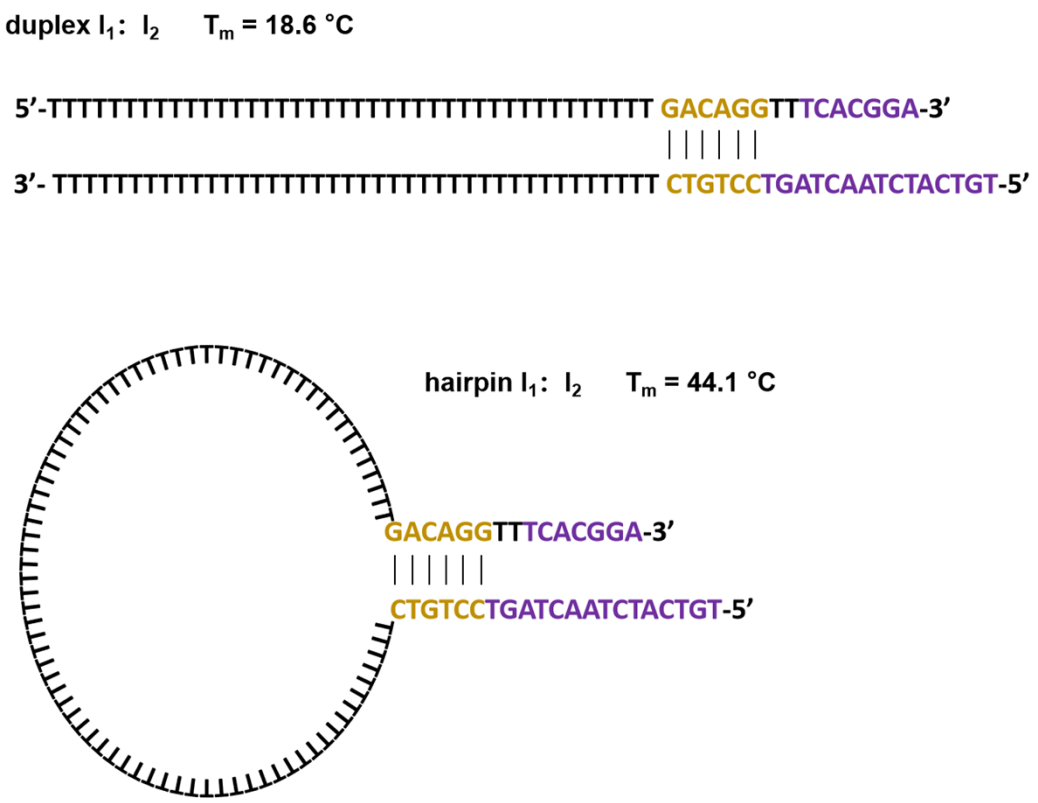

Fig. S6. The T_m values were estimated by UNAFold under a condition of 10 mM NaCl and 12.5 mM $MgCl_2$. The hairpin I_1:I_2 with 6-base stem domain and 80-base poly-thymine loop domain was used to simulate the affinity complex.

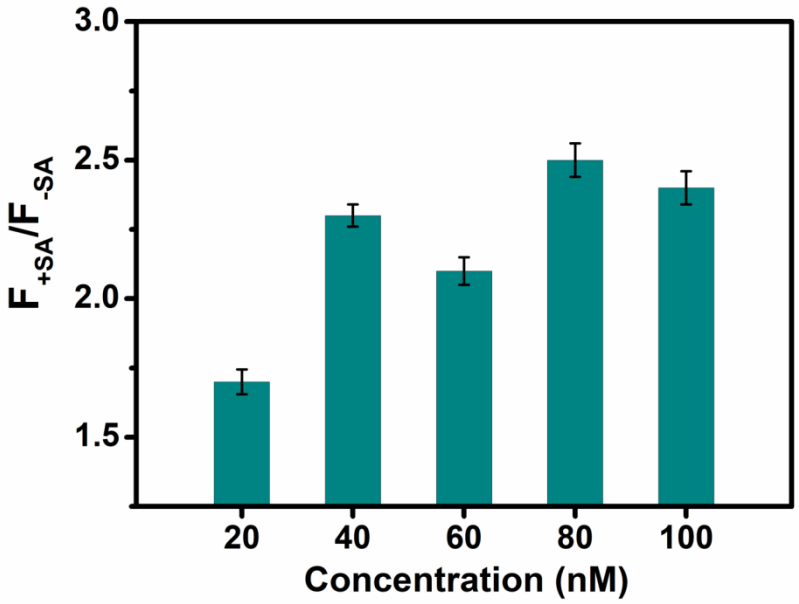

Fig. S7. Signal-to-background ratios of SA-responsive CCHA reaction under 3 nM SA, 30 nM split initiators (I_{b1} and I_{b2}), and different concentrations of hairpin trimers (H_1^Y and H_2^Y) in 1x HEPES buffer at 37 °C for 4 h.

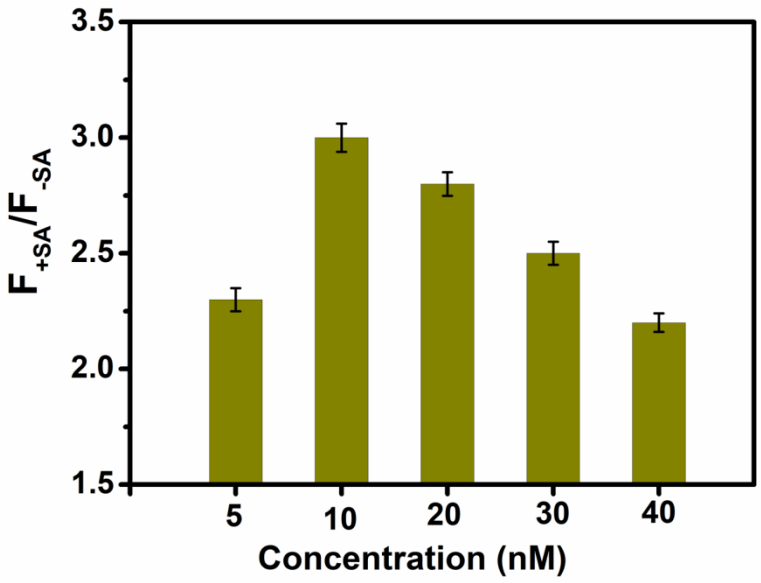

Fig. S8. Signal-to-background ratios of SA-responsive CCHA reaction in the presence of 3 nM SA, 80 nM hairpin trimers (H_1^Y and H_2^Y), and increasing concentrations of split initiators (I_{b1} and I_{b2}) in 1x HEPES buffer at 37 °C for 4 h.

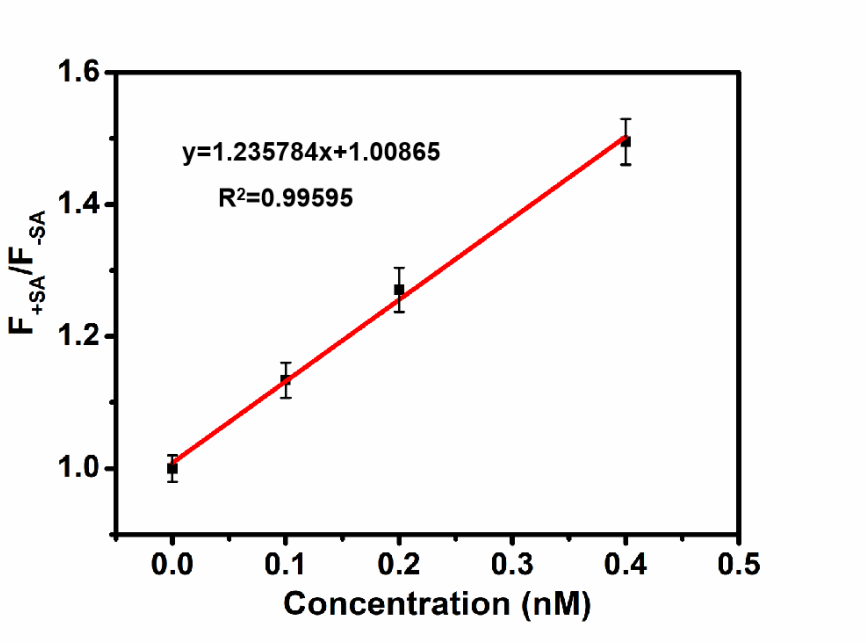

Fig. S9. Linear fitting curve of the fluorescence signal change versus the concentrations of SA.

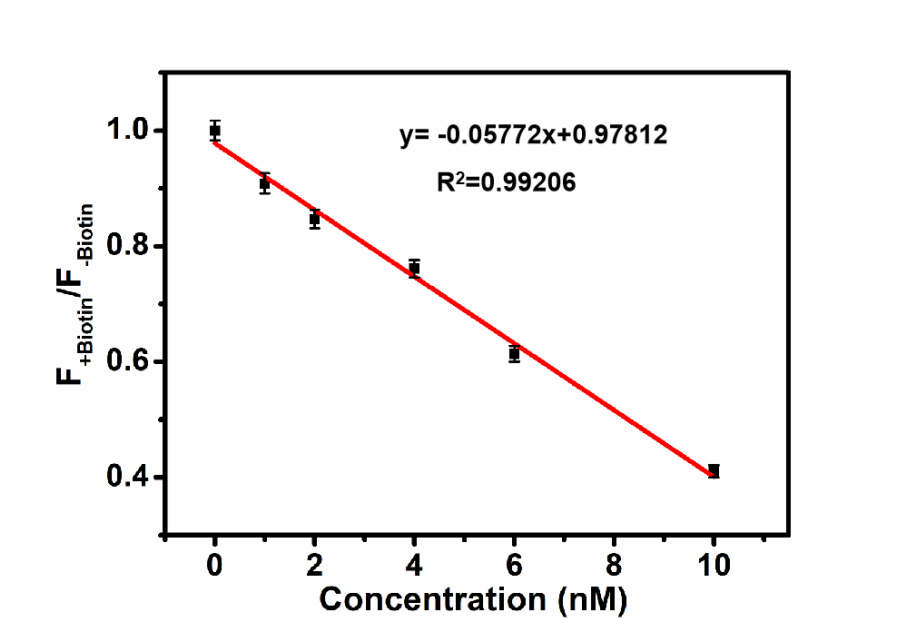

Fig. S10. Linear fitting curve of the fluorescence signal change versus the concentrations of biotin.

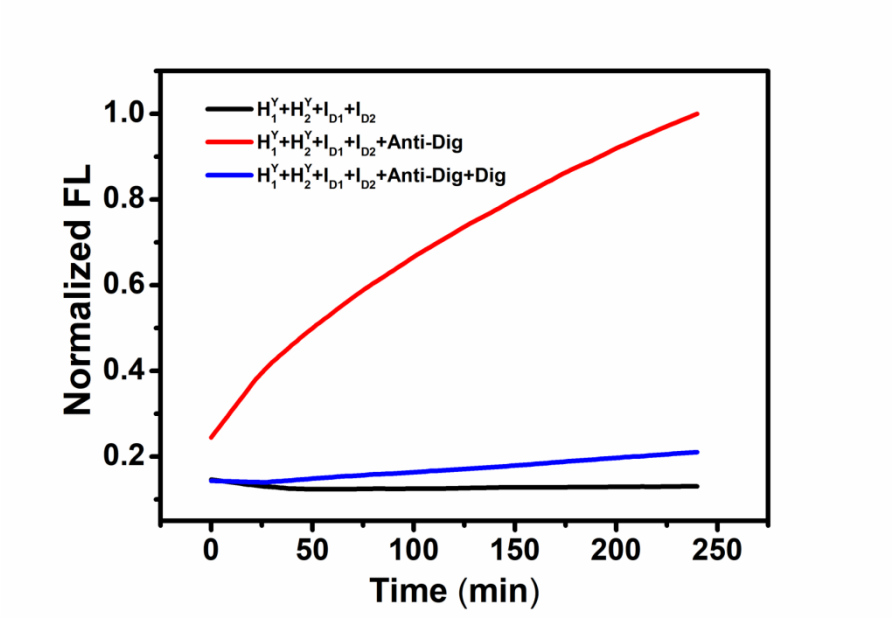

Fig. S11. Real-time fluorescence signal of programmable CCHA reaction under different experiment conditions, the emission wavelength was fixed at 520 nm with 480 nm excitation wavelength.

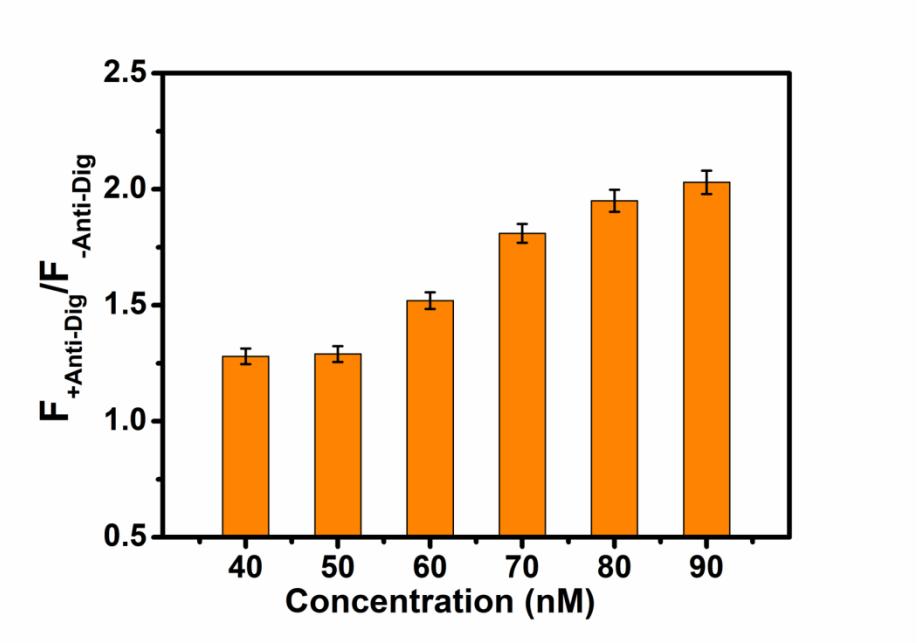

Fig. S12. Signal-to-background ratios of Anti-Dig antibody initiated CCHA reaction under varying concentrations of split initiators (I_{D1} and I_{D2}) plus 100 nM Anti-Dig antibody, 80 nM hairpin trimers (H_1^Y and H_2^Y) in 1x HEPES buffer at 37 °C for 4 h.

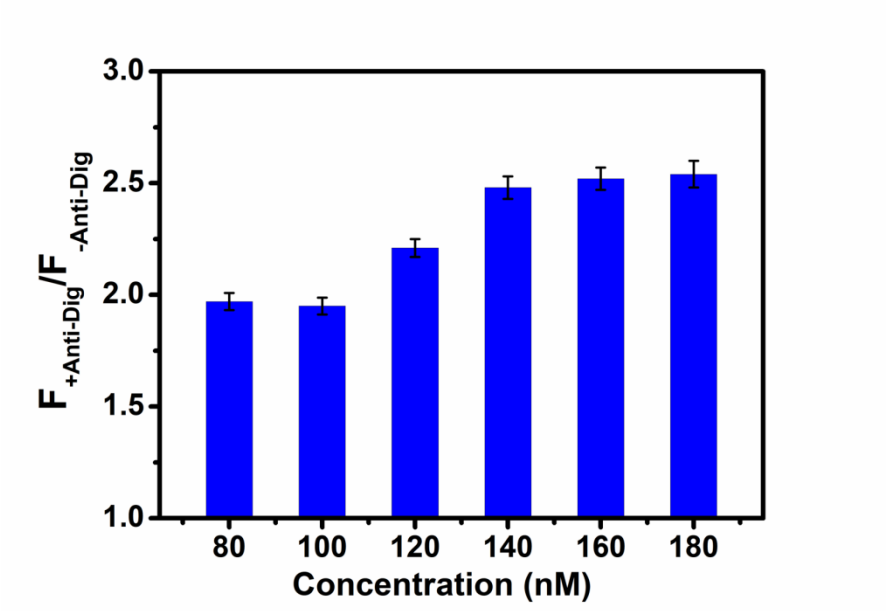

Fig. S13. Signal-to-background ratios of Anti-Dig antibody triggered CCHA reaction with varying concentrations of hairpin trimers (H_1^Y and H_2^Y) plus 100 nM Anti-Dig antibody, 80 nM split initiators (I_{D1} and I_{D2}) in 1x HEPES buffer at 37 °C for 4 h.

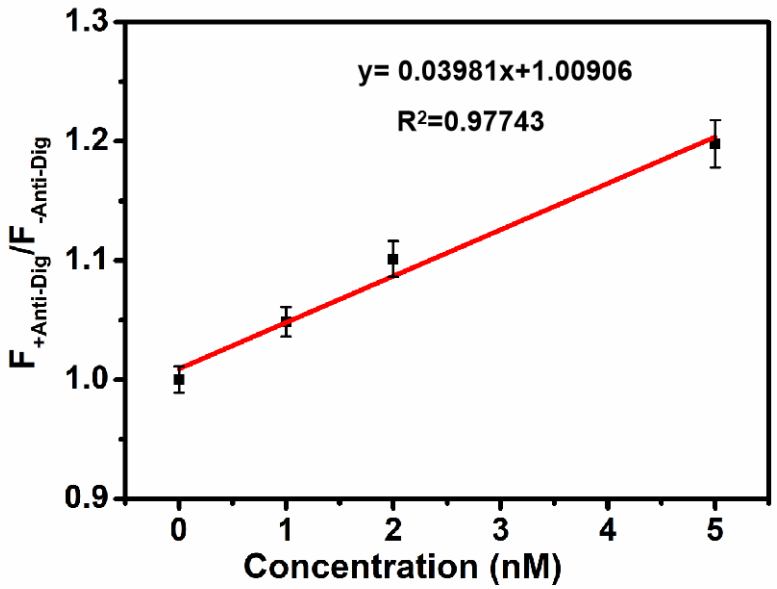

Fig. S14. Linear fitting curve of the fluorescence signal change versus the concentrations of Anti-Dig antibody.

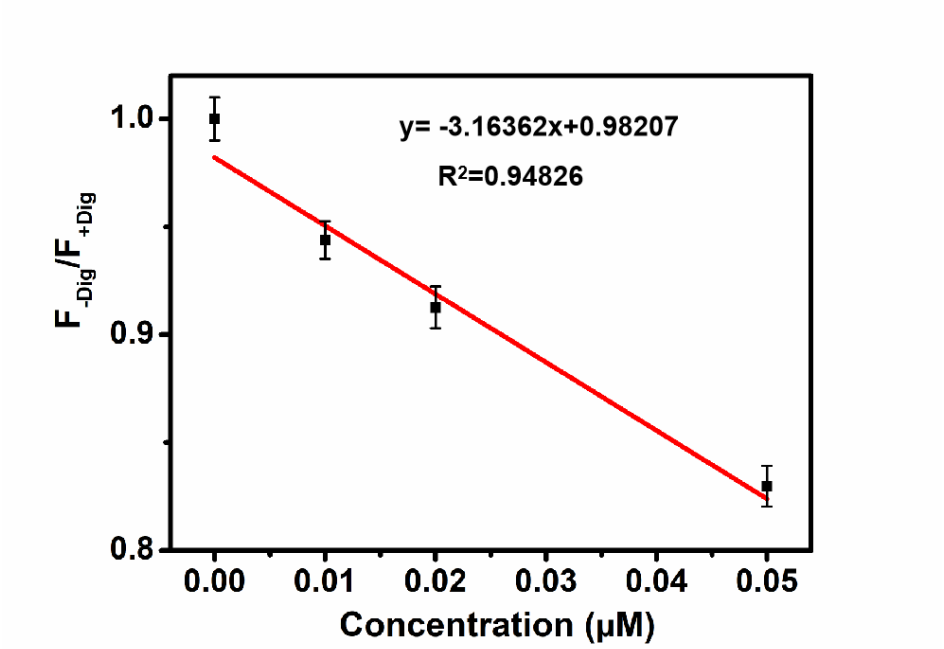

Fig. S15. Linear fitting curve of the fluorescence signal change versus the concentrations of digoxigenin.

Table S2. Recovery experiment of proteins, SA (number 1 to 3) and Anti-Dig antibody (number 4 to 6), in 10 % human serum sample.

Samples	Spiked Protein (nM)	Found Protein (nM)	Recovery (%)	RSD (n=3, %)
1	1	1.10	110.0	4.2
2	2.5	2.46	98.4	4.8
3	4.5	4.59	102.0	3.7
4	25	24.59	98.4	3.8
5	60	63.57	106.0	4.2
6	120	122.04	101.7	3.9

Table S3. Recovery experiment of small molecules, biotin (number 1 to 3) and Dig (number 4 to 6), in 10 % human serum sample.

Samples	Spiked Small Molecule	Found Small Molecule	Recovery (%)	RSD (n=3, %)
1	1 nM	1.07 nM	107.0	3.6
2	2 nM	2.20 nM	110.0	4.1
3	5 nM	4.68 nM	93.6	2.9
4	0.2 μM	0.22 μM	110.0	4.9
5	0.5 μM	0.47 μM	94.0	4.0
6	0.8 μM	0.84 μM	105.0	3.5

Table S4. Comparison of the detection performance toward proteins with different methods.

Technique	Target	Detection limit	Sensing strategy	Reference
Fluorescence	Streptavidin	0.47 nM	Magnetic separation and copper nanoclusters	1
Fluorescence	Streptavidin	1.07 nM	Sterically and allosterically tunable hybridization chain	2
Fluorescence	Streptavidin	2.93 nM	Protein-induced fluorescence enhance	3
Fluorescence	Streptavidin	0.27 nM	Sterically tunable nucleic acid hyperbranched rolling circle amplification	4
Electrochemistry	Streptavidin	3.67	Nucleic Acid Nanostructure	5
Electrochemistry	Anti-Dig antibody	1.23	Nucleic Acid Nanostructure	5
Electrochemistry	Anti-Dig antibody	9 nM	Multiplexed DNA Circuits	6
Fluorescence	Anti-Dig antibody	5.6 nM	Steric hindrance inhibition of the DNA strand displacement	7
Electrochemilum inescence	Anti-Dig antibody	0.72 nM	S-doped yttrium oxide ultrathin nanosheets	8
Fluorescence	streptavidin	48.8 pM	Programmable catalytic molecular nanomachine	This work
Fluorescence	Anti-Dig antibody	0.85 nM	Programmable catalytic molecular nanomachine	This work

Table S5. Comparison of the detection performance toward small molecules with different methods.

Technique	Target	Detection limit	Sensing strategy	Reference
Fluorescence	Biotin	3.1 nM	Magnetic separation and copper nanoclusters	1
Electrochemistry	Biotin	3.57 μM	Nucleic Acid Nanostructure	5
Fluorescence	Biotin	13 nM	Antibody-Bridged Beacon	9
Electrochemistry	Dig	177 nM	Nucleic Acid Nanostructure	5
Fluorescence	Dig	28 nM	Antibody-Bridged Beacon	9
Fluorescence	Dig	60.5 nM	Small-MoleculeLinked Hybridization Chain Reaction	10
Electrochemistry	Dig	10 nM	DNA-Based Immunoassay	11
Fluorescence	Biotin	0.89 nM	Programmable catalytic molecular nanomachine	This work
Fluorescence	Dig	9.5 nM	Programmable catalytic molecular nanomachine	This work

References

1 J. Cao, W. Wang, B. Bo, X. Mao, K. Wang and X. Zhu, *Biosens. Bioelectron*., 2017, **90**, 534-541.

2 F. Ban, H. Shi, C. Feng, X. Mao, Y. Yin and X. Zhu, *Biosens. Bioelectron*., 2016, **86**, 219-224.

3 H. Kim, C. Y. Lee, J. Song, J. Yoon, K. S. Park and H. G. Park, *RSC Adv.*, 2018, **8**, 39913-39917.

4 H. Shi, X. Mao, X. Chen, Z. Wang, K. Wang and X. Zhu, *Biosens. Bioelectron*., 2017, **91**, 136-142.

5 Somasundaram and C. J. Easley, *J. Am. Chem. Soc.,* 2019, **141**, 11721-11726.

6 3S. Bracaglia, S. Ranallo, K. W. Plaxco, and F. Ricci, *ACS Sens*., 2021, 6, 2442-2448.

7 Y. Peng, X. Li, R. Yuan and Y. Xiang, *Chem. Commun.*, 2016, **52**, 12586-12589.

8 H. Gao, S. Liu, Z. Wang, L. Si and Z. Dai, *Analyst.*, 2018, **143**, 2997-3000.

9 X. Yan, X. C. Le and H. Zhang, *Anal. Chem*., 2018, **90**, 9667-9672.

10 M. Hansen-Bruhn, L. D. F. Nielsen and K. V. Gothelf, *ACS Sens.*, 2018, **3**, 1706-1711.

11 S. S. Mahshid, F. Ricci, S. O. Kelley and A. Vallée-Bélisle, *ACS Sens.*, 2017, **2**, 718-723.